Design Codes for High Power Vacuum Electronic Devices [1]

A. N. Vlasov, T. M. Antonsen Jr,* I. A. Chernyavskiy, S. J. Cooke**, K. T. Nguyen*** , B. Levush**

Science Applications International Corporation, McLean, VA 22102, USA, (301) 405-1627, (301) 405-1678, Alexander.N.Vlasov@saic.com
** Institute for Research in Electronic and Applied Physics, University of Maryland, College Park, MD 20742, USA*
*** Naval Research Laboratory, Washington DC 20375, USA*
**** Beam- Wave Research Inc., Silver Spring, MD 20905, USA*

Abstract –Highly efficient codes MAGY and TESLA have been developed to support design of high power vacuum electronic devices. The codes are capable of simulating vacuum electronic devices such as gyrotrons, gyro frequency multipliers, gyro TWTs, gyro BWOs, relativistic BWOs and TWTs, cavity type klystrons, extended interaction klystrons (EIK), multiple beam klystrons (MBK).

1. Introduction

Effective design codes MAGY (MAryland GYrotron code) [1,2] and TESLA (Telegraphist's Equations Solution for Linear beam Amplifiers) [3] have been developed at NRL (Naval Research Laboratory), UMD (University of Maryland) and SAIC (Science Applications International Corporation) to support efforts of the US vacuum electronic industry in development of new vacuum electronic devices with improved characteristics.

The codes provide self-consistent time dependent solution of field equations together with 3D relativistic equations of motions for electron beam for wide variety of slow and fast wave structures. The codes are hybrid codes in accordance with classification introduced in [4]. They combine accuracy of PIC (Particles in Cell) codes and effectiveness of parametric codes.

The codes are effective because selected compact electromagnetic (EM) field representation allows fast solution of field equations without limitations for time step common for PIC codes. Independent selection of time step and spatial grid size gives more capabilities for the codes to get detailed information about EM field and interaction between EM field and an electron beam. Typical running time for MAGY and TESLA codes on standard PC computers is from tens of seconds to several hours for different task and different levels of complexity of structures under simulations.

The codes were been verified by comparison with prediction of PIC code MAGIC [5], validated by comparison with experimental measurements and used for modeling and design many gyro-devices (gyrotrons, gyro-klystrons, gyro frequency multipliers, gyro-BWO, gyro-TWT) and klystrons, multiple beam klystrons (MBK), extended interaction klystrons (EIK).

2. Basic Model

For vacuum electronic devices with relatively narrow instantaneous spectrum of a signal we can use simplified equations for electromagnetic fields providing accurate and effective way to find electromagnetic fields inside a beam tunnel.

The electromagnetic field in the beam region is represented as a sum of transverse and longitudinal parts:

$$\mathbf{E}(\mathbf{r},t) = \mathrm{Re}\left\{\sum_n \left[(\mathbf{E}_\mathbf{T}^n(\mathbf{r},t) + E_z^n(\mathbf{r},t)\mathbf{i}_\mathbf{z}) e^{-i\omega_n t} \right]\right\}, \quad (1)$$

$$\mathbf{B}(\mathbf{r},t) = \mathrm{Re}\left\{\sum_n \left[(\mathbf{B}_\mathbf{T}^n(\mathbf{r},t) + B_z^n(\mathbf{r},t)\mathbf{i}_\mathbf{z}) e^{-i\omega_n t} \right]\right\}, \quad (2)$$

where $\mathbf{E_T}$, $\mathbf{B_T}$ are the complex amplitudes of the transverse electric and magnetic fields, E_z , B_z are the complex amplitudes of the longitudinal field components, ω_n are carrier frequencies, and $\mathbf{i_z}$ is a unit vector directed along the z axis. The complex field vectors $\mathbf{E_T}$ and $\mathbf{B_T}$ as well as E_z and B_z are assumed to be slowly varying functions of time. The transverse fields are represented at each axial location as a sum of TM, TE and TEM modes of a waveguide with a transverse cross-section equal to the local transverse cross section of the beam region,

$$\mathbf{E}_\mathrm{T}^n = \sum_k \left(V_k'^n(z,t)\mathbf{e}_\mathbf{k}'(\mathbf{r}_\mathbf{T},z) + V_k''^n(z,t)\mathbf{e}_k''(\mathbf{r}_\mathbf{T},z) \right), \quad (3)$$

$$\mathbf{B}_\mathbf{T}^n = \sum_k \left(I_k'^n(z,t)\mathbf{b}_\mathbf{k}'(\mathbf{r}_\mathbf{T},z) + I_k''^n(z,t)\mathbf{b}_k''(\mathbf{r}_\mathbf{T},z) \right). \quad (4)$$

Here the primed variables refer to TM modes and the double primed variables refer to TE modes. The amplitudes V_k' , V_k'' , I_k' and I_k'' depend slowly on time and arbitrarily on the axial coordinate z. The two sets of eigenfunctions of the local transverse cross-section are introduced as follows:

[1] The work was supported by US Office of Naval Research

$$\mathbf{e}'_k = \nabla_\perp \Psi_k , \tag{5}$$

$$\mathbf{b}'_k = \mathbf{e_z} \times \mathbf{e}'_k , \tag{6}$$

where

$$\Delta\Psi_k + k'^2_{c,k}\Psi_k = 0, \qquad \Psi_k\big|_C = 0 \tag{7}$$

describing TM modes, and

$$\mathbf{b}''_k = \nabla_\perp \Phi_k , \tag{8}$$

$$\mathbf{e}''_k = \mathbf{b}''_k \times \mathbf{e}_z , \tag{9}$$

where

$$\Delta\Phi_k + k''^2_{c,k}\Phi_k = 0, \qquad \mathbf{n}\cdot\nabla\Phi_k\big|_C = 0 \tag{10}$$

describing TE modes.

Here C is the curve defining the boundary of local cross-section $S_\perp$ in which the field is represented; **n** is outward normal from this curve.

The longitudinal components of electromagnetic fields are expressed from the transverse components (3),(4) and Fourier components of bunched electron current j_z by using Maxwell's equations:

$$i\frac{\omega_n}{c}B^n_z = \nabla_\perp \cdot \left(\mathbf{E}^n_\mathbf{T} \times \mathbf{i_z}\right), \tag{11}$$

$$i\frac{\omega_n}{c}E^n_z = \frac{4\pi}{c}j^n_z - \nabla_\perp \cdot \left(\mathbf{B}^n_\mathbf{T} \times \mathbf{i_z}\right) \tag{12}$$

where $j_z{}^n$ is complex Fourier component of beam current at frequency ω_n.

The electromagnetic field representation (1), (2), (3), (4), (11), (12) allows to get complete solution of Maxwell's equations under assumption of slow varying complex field amplitudes in time. For selected electromagnetic field representation the Maxwell's equations can be reduced to matrix Telegraphist's Equations with respect to complex amplitudes of the modes of local cross-section:

$$0 = \widetilde{\Delta}^n_k I^n_k - \frac{\partial V^n_k}{\partial z} + \sum_l K_{l,k} V^n_l - S^n_{z,k} + \int_C dl\, \mathbf{n}\cdot\mathbf{e}^*_\mathbf{k}\left(E^n_z + r'_w \mathbf{n}\cdot\mathbf{E}^n_\perp\right) \tag{13}$$

$$0 = \widetilde{\Gamma}^n_k V^n_k - \frac{\partial I^n_k}{\partial z} + \sum_l K_{k,l} I^n_l - S^n_{T,k} - \frac{c}{i\omega_n}\int_C dl\, \mathbf{n}\cdot\left(\mathbf{E}^n_\perp \times \mathbf{i_z}\right)\nabla_\perp \cdot \mathbf{b}^*_\mathbf{k} . \tag{14}$$

where r'_w is derivative of r_w with respect to the axial variable z. Coupling matrix $K_{l,k}$ describes mode transformation due to variations of wall radius r_w. Operators $\widetilde{\Delta}^n_k$ and $\widetilde{\Gamma}^n_k$ determine the axial propagation and time evolution for the wavegide modes:

$$\widetilde{\Delta}^n_k = \begin{cases} i\dfrac{\omega_n}{c}\left(1 - \dfrac{k'^2_{c,k}}{(\omega_n/c)^2}\right) - \dfrac{2}{c}\dfrac{\partial}{\partial t} & \text{for TM modes} \\ i\dfrac{\omega_n}{c} & \text{for TE modes} \end{cases} \tag{15}$$

$$\widetilde{\Gamma}^n_k = \begin{cases} i\dfrac{\omega_n}{c} & \text{for TM modes} \\ i\dfrac{\omega_n}{c}\left(1 - \dfrac{k''^2_{c,k}}{(\omega_n/c)^2}\right) - \dfrac{2}{c}\dfrac{\partial}{\partial t} & \text{for TE modes} \end{cases} \tag{16}$$

The quantities $S_{z,k}$ and $S_{T,k}$ are source terms describing presence of an electron beam inside beam tunnel:

$$S^n_{z,k} = \frac{4\pi}{i\omega}\int_{S_\perp} da\, j^n_z\ \nabla_\perp \cdot \mathbf{e}^*_\mathbf{k} \tag{17}$$

$$S^n_{T,k} = \frac{4\pi}{c}\int_{S_\perp} da\, \mathbf{j}^n_\mathbf{T} \cdot \mathbf{e}^*_\mathbf{k} \tag{18}$$

where j^n_z and $\mathbf{j}^n_\mathbf{T}$ are the Fourier components at frequency ω_n of the beam current.

The filed representation works very well for electromagnetic fields inside beam tunnel for the case when the radius of boundary can be represented as a single valued function of z. However, for structures with external resonators it is not evident that outer boundary of the structure under simulation can be expressed as a single valued function of z. The schematic picture of a device with external resonator is presented in Fig. 1.

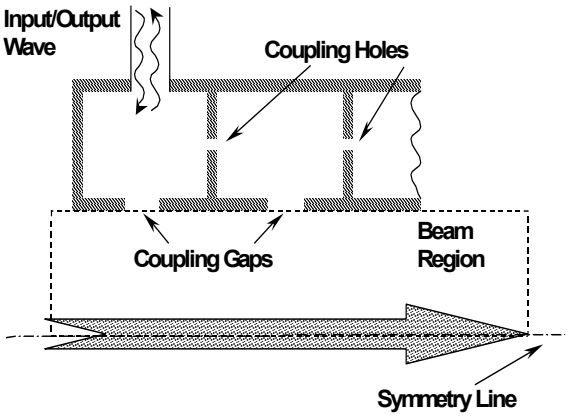

Fig.1. Schematic picture of electron device with external cavities

The field model has been extended to allow simulations of structures with external cavities. The extended model is based on decomposition of whole volume of electron device into two parts: beam region or beam tunnel and external cavity region coupled through coupling gaps. The RF field continuation boundary conditions are applied on coupling gap.

The fields inside external cavities are represented as a superposition of cavity modes with time dependent amplitudes,

$$\mathbf{E} = \mathrm{Re}\left(\sum_{s,n} V^n_s(t)\,\mathbf{e_s}\, e^{-i\omega_n t}\right), \tag{19}$$

$$\mathbf{B} = \mathrm{Re}\left(\sum_{s,n} I_s^n(t)\mathbf{b}_\mathbf{s}\, e^{-i\omega_n t} \right) \quad (20)$$

The representation will be made independently in each cavity, so cavity index is omitted in expressions (19) and (20). The fields of external resonator's eigenmodes $\mathbf{e_s}$ and $\mathbf{b_s}$ are satisfied homogeneous Maxwell's equations with perfect conducting boundary conditions on metal surfaces and the perfect magnetic boundary conditions on the coupling gap at r=r_w.

Resonator's evolution equations are derived from Maxwell's equations:

$$\frac{dV_s^n}{dt} = -i\omega_s I_s^n + i\omega_n V_s^n - \omega_s \int_{S_{gap}} \mathbf{e}_\mathbf{s}^* \times \mathbf{B}^n \cdot \mathbf{n}_c \, dS \quad (21)$$

$$\frac{dI_s^n}{dt} = -i\omega_s V_s^n + i\omega_n I_s^n - \omega_s \int_{S_{holes+slots}} \mathbf{E}^n \times \mathbf{b}_\mathbf{s}^* \cdot \mathbf{n}_c \, dS - \omega_s \sum_{s'} L_{s,s'} I_{s'}^n \quad (22)$$

where S_{gap} is the coupling gap surface and $S_{hole+slotes}$ is the surface of slots and holes. The effect of non-zero surface impedance of the cavity and presence of lossy elements inside cavity is given by

$$L_{s,s'} = \int_{S_{wall}} Z_s \left(\mathbf{n}_c \times \mathbf{b}_\mathbf{s}^*\right) \cdot \left(\mathbf{n}_c \times \mathbf{b}_{\mathbf{s}'}\right) dS \quad (23)$$

The resonator's eigenmodes used in TESLA field model are different from actual eigenmodes because the actual eigenmodes are found for whole resonator volume including beam tunnel region while TESLA eigenmodes are found with perfect magnetic boundary conditions on the coupling gap.

The surface integrals in telegraphist's equations (13), (14) are calculated for selected resonator's field representation. The final version of Telegraphist's equations is as follows:

$$0 = \tilde{\Delta}_k^n I_k^n - \frac{\partial V_k^n}{\partial z} + \sum_l K_{l,k} V_l^n - S_{z,k}^n + \sum_s K^{*res}_{s,k} V_s^n \quad (24)$$

$$0 = \tilde{\Gamma}_k^n V_k^n + \frac{\partial I_k^n}{\partial z} + \sum_l K_{k,l} I_l^n + S_{T,k}^n - \frac{c}{i\omega_n} \sum_s M^{*res}_{s,k} V_s^n \,. \quad (25)$$

where resonator's coupling matrixes are

$$K_{s,k}^{res} = \oint_\mathbf{C} \left(\mathbf{e_k} \cdot \mathbf{n}\right) e_{s,z}^* \, dl \,, \quad (26)$$

$$M_{s,k}^{res} = \oint_C \left(\nabla_\perp \cdot \mathbf{b}_k''\right) \mathbf{e}_\mathbf{s}^* \times \left(\mathbf{i_z} \times \mathbf{n}\right) dl \quad (27)$$

3. Numerical implementation and convergence

The selected electromagnetic field representation (1) - (4), (11),(12) allows to reduce 3D electromagnetic problem to set of 1D problems for different azimuthal indexes. In the case of axially symmetric electromagnetic structure the fields with different azimuthal indexes are independent.

However, convergence of electromagnetic field solution with respect to number of modes included in simulations are strongly depends on boundary conditions on the bounding wall. For the case of perfectly conducting boundary conditions the basic electromagnetic model can be used. For the case of conducting walls or presence of external resonator the basic model should be extended to avoid differentiation of non-uniform convergent series.

The problem is illustrated in Fig.2 where radial dependence of actual electromagnetic field in structure with finite conductivity of walls. The actual electromagnetic field has a non-zero value on wall, while all fields of basic functions go to zero. The same problem appears in the case of external resonators coupled to the beam tunnel through the gap. The electromagnetic field with non-zero value on the wall should be represented as a sum of basis functions with zero fields on the wall.

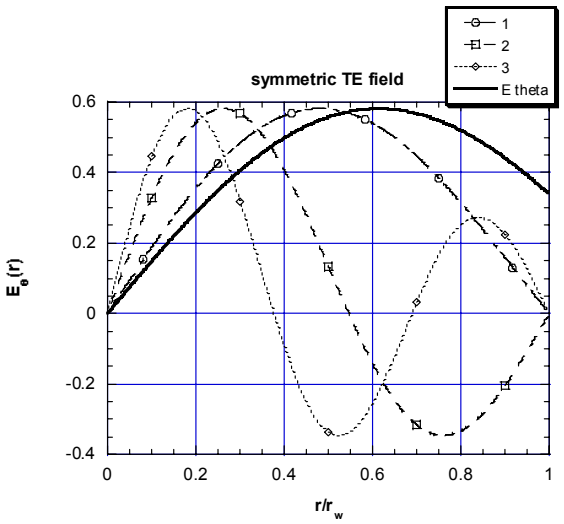

Fig. 2. The radial distribution of actual E_θ field and fields of first three basis functions for structure with finite wall conductivity

To avoid differentiation of non-uniformly convergent series in (11), (12) the basic electromagnetic field model has been extended to deal with infinite number of basis functions in the regions with non-zero electromagnetic fields on the boundary. The basic idea of non-uniformly convergent series treatment is to re-express longitudinal components of electromagnetic fields in the way which does not require series differentiation and do not truncate the series, but treat infinite series tails analytically.

This approach leads to modifications of Telegraphist's equations for the cases of finite surface impedance of beam tunnel walls [12] and for modification of resonator's excitation equations in presence of external resonators [4].

$$\frac{dV_s^n}{dt} = -i\omega_s I_s^n + i\omega_n V_s^n - \omega_s \int_{z_{\min}}^{z_{\max}} \sum_k K_{s,k}^{res} I_k^n dz - \omega_s \frac{4\pi}{c} \int_{z_{\min}}^{z_{\max}} dz \int_{S_\perp} \mathbf{j}_{n\omega} \cdot \mathbf{e}_s^{*\,\mathbf{gap},n} dS + \omega_s \sum_{s'} C_{s,s'}^{self} V_{s'}^n, \quad (28)$$

$$\frac{dI_s^n}{dt} = -i\omega_s V_s^n + i\omega_n I_s^n - \omega_s S^{hole} - \omega_s \sum_{s'} L_{s,s'} I_{s'}^n \quad (29)$$

Modified resonators' equations contain $C_{s,s'}^{self}$ term describing the effect of infinite number of basis functions taking into account to provide convergence of field solution in the gap region. To identify properties of actual resonator's modes with TESLA modes a tuning procedure has been introduced into TESLA code.

4. Resent development of the codes

Resent activity in development of the models and the codes is aimed to extend codes for simulations new vacuum electronic devices with improved characteristics (bandwidth and output power). It is commonly that devices with improved characteristics employ complex electrodynamic structures as well as multi beam electron beams. The price what should be paid for improved characteristics is more complex and more complex and time consuming designing process. Efficient and accurate computer codes are very useful tool for extended devices design.

Design code TESLA has been extended to simulate klystrons with two gap resonators. Two gap resonators provide better coupling between electron beam and resonators' fields and allow effective interaction between electron beam and resonators' fields at low values of quality factors. However in two gap resonators two closely spaced modes can interact with the electron beam.

Note, that the resonator's modes used in TESLA model are different from the actual resonator's modes. In the case of two gap two mode resonator the TESLA modes are coupled to each other due to presence of the gap between cavity volume and the beam tunnel and slots between resonator volume and input wavegide. Basic TESLA model allows simulating two gap two resonator fields under assumption that the electromagnetic fields are symmetric with respect to center plane of the resonator. In this case the electromagnetic fields of two modes are orthogonal inside the beam tunnel and matrix $C_{s,s'}^{self}$ are diagonal.

However, the resonator's fields become non-orthogonal if resonator is loaded by lossy elements non-symmetrically or coupling to input/output circuits is made non-symmetric with respect to the center plane. TESLA resonator's tuning algorithm has been modified to find appropriate parameters of TESLA modes in the case when they are non-orthogonal inside beam tunnel.

The results of TESLA code calculations for two gap two mode resonators with non-symmetric loading agree well with predictions of electromagnetic code HFSS [13] and PIC code MAGIC [5].

References

[1] S.C.Cai, T.M. Antonsen Jr., G.Saraph, and B. Levush, Int. J. Electronics, **72**, 759, (1992).

[2] M. Botton, T.M. Antonsen Jr., B. Levush, K.T. Nguyen, and A.N. Vlasov , IEEE Trans on Plasma Science, **26**, 3, 882, (1998).

[3] A.N.Vlasov, T.M. Antonsen Jr., D.P.Chernin, B. Levush, and E.L.Wright, IEEE Trans on Plasma Science, **30**, 3, 1277, (2002).

[4] T.M. Antonsen Jr., A.A.Mondelli, B.Levush, J.P.Verboncoeur, and C.K.Birsall, Proceedings of the IEEE, **87**, 5, 804, (1999).

[5] B. Goplen, L. Ludeking, D. Smithe, and G. Warren, Comput. Phys. Commun., **87**, 54, (1995).

[6] S.J.Cooke, K.T.Nguyen, A.N.Vlasov, T.M. Antonsen Jr., B.Levush, T.A.Hargreaves, and M.F.Kirshner, IEEE Trans on Plasma Science, **32**, 3, 1136, (2004).

[7] G.S.Nusinovich, O.V.Sinitsyn, L.Velikovich, M.Yedulla, T.M. Antonsen Jr., A.N.Vlasov, S.R.Cauffman, and K.Felch, IEEE Trans on Plasma Science, **32**, 3, 841, (2004).

[8] K.T.Nguyen, B.Levush, T.M. Antonsen Jr., M.Botton, M.Blank,J.P.Calame, and B.G.Danly, IEEE Trans on Plasma Science, **28**, 3, 867, (2000).

[9] G.S.Nusinovich, T.M. Antonsen Jr., A.N.Vlasov, Phys. Rev. Letters, **87**, 21, 218301/1-4, (2001)

[10] M.Garven, J.P.Calame, B.G.Danly, K.T.Nguyen, B.Levush, F.N.Wood, and D.E.Pershing, IEEE Trans on Plasma Science, **30**, 3, 885, (2002).

[11] K.T.Nguyen, D.K.Abe, D.E.Pershing, B.Levush, E.L.Wright, H.Bohlen, A.Staprans, L.Zitelli, D.Smithe, J.A.Pasour, A.N.Vlasov, T.M. Antonsen Jr., K.Eppley, and J.J.Petillo, IEEE Trans on Plasma Science, **32**, 3, 1119, (2004).

[12] A.N.Vlasov and T.M. Antonsen Jr., IEEE Trans. on Electron Devices, **48**, 1, 45, (2001).

[13] HFSS is a product of Ansoft Corporation available at www.ansoft.com/product/hf/hfss